Regulation of the Hippo pathway by phosphatidic acid-mediated lipid-protein interaction

Han Han, Ruxi Qi, Jeff Jiajing Zhou, Albert Paul Ta, Bing Yang, Hiroki J Nakaoka, Gayoung Seo, Kun-Liang Guan, Ray Luo and Wenqi Wang

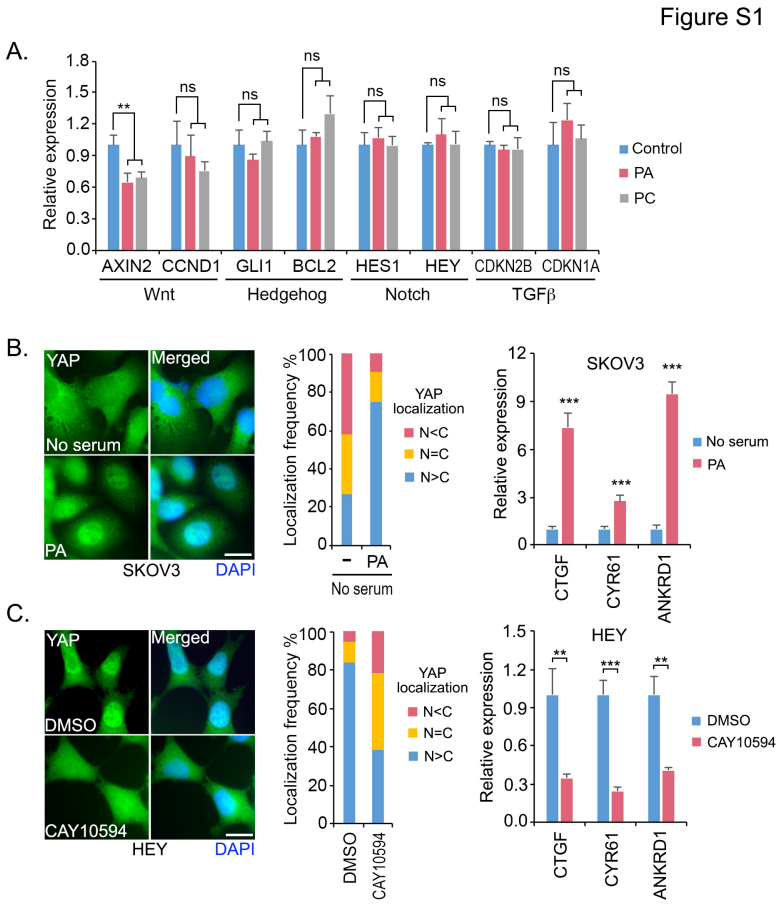

Figure S1. PA treatment activates YAP. (This figure is related to Figure 1)

(**A**) Role of PA in regulation of different signaling pathways. The gene transcripts for the indicated pathways were detected by quantitative PCR in serum-starved cells under lipid treatment (100 μM) for 2 hours, and normalized (mean ± s.d., n = 3 biological replicates). ** $p <$ 0.01. ns, no significance.

(**B**) PA activates YAP in SKOV3 cells. Serum-starved SKOV3 cells were subjected to PA (100 μM) treatment for 30 min and YAP localization was detected by immunofluorescent staining. Nuclei were visualized by DAPI. YAP-regulated gene transcripts (*CTGF*, *CYR61* and *ANKRD1*) were detected by quantitative PCR in serum-starved cells under PA (100 μM) treatment for 2 hours, and normalized (mean ± s.d., n = 3 biological replicates). *** $p < 0.001$. Scale bar, 20 μm.

(**C**) Inhibition of PLD-mediated PA production inactivates YAP in HEY cells. HEY cells were subjected to PLD inhibitor CAY10594 (20 μM) treatment for 2 hours at normal culture condition. YAP localization was detected by immunofluorescent staining. Nuclei were visualized by DAPI. YAP-regulated gene transcripts (*CTGF*, *CYR61* and *ANKRD1*) were detected by quantitative PCR in cells under DMSO or CAY10594 (20 μM) treatment for 4 hours, and normalized (mean ± s.d., n = 3 biological replicates). ** $p < 0.01$. *** $p < 0.001$. Scale bar, 20 μm.

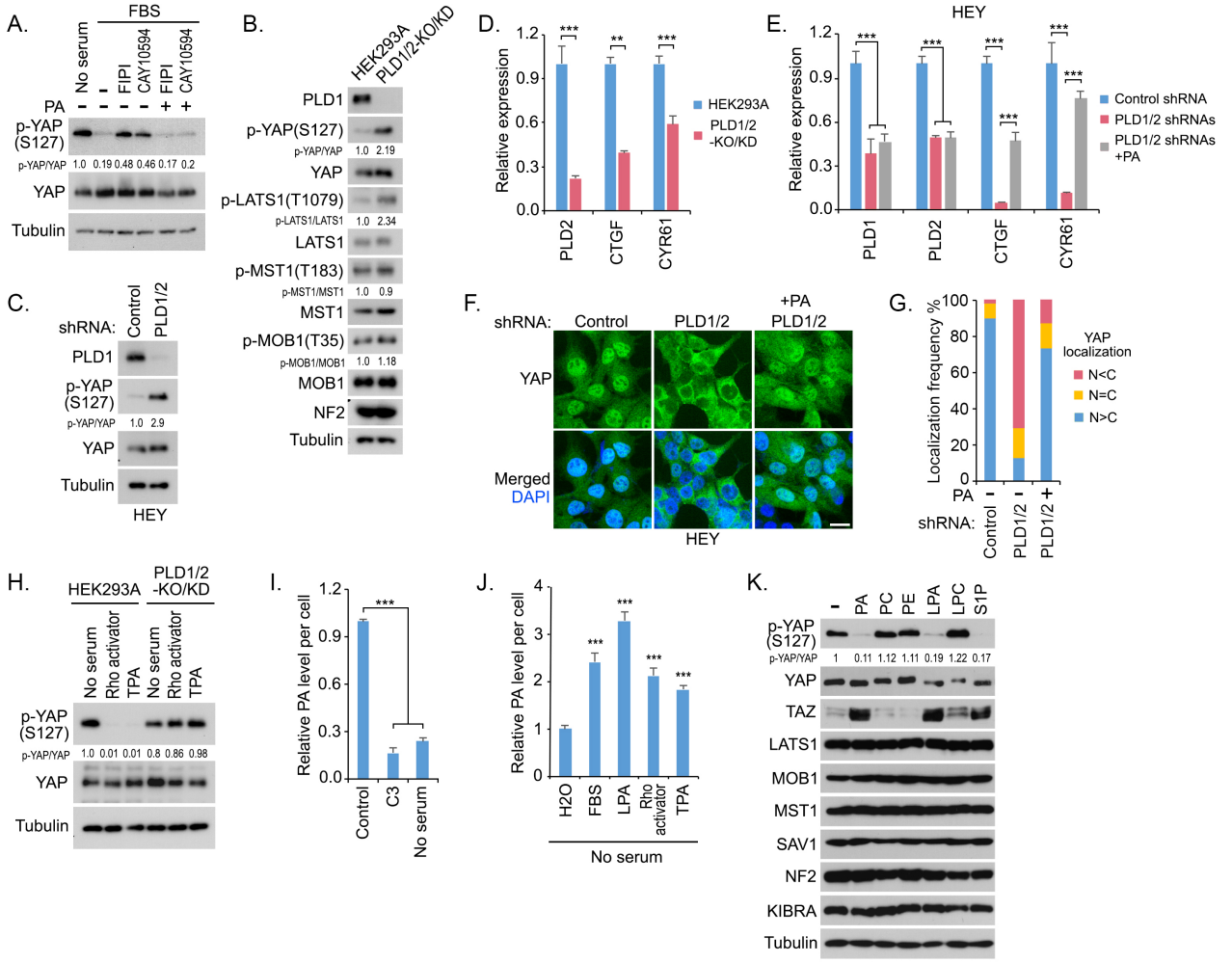

Figure S2. PLD-PA lipid signaling positively regulates YAP. (This figure is related to Figures 1, 2 and 3)

(**A**) Inhibition of PLD-mediated PA production increases YAP phosphorylation under serum-treated condition. Serum-starved HEK293A cells were pretreated with 30 μM FIPI or 20 μM CAY10594 for 30 min and subjected to serum treatment for 1 hour. PA treatment (100 μM) was performed for 30 min. Western blotting was performed with indicated antibodies.

(**B**) Loss of PLD1/2 increases YAP phosphorylation in HEK293A cells. PLD1 KO cells were generated using CRISPR-Cas9 system and further transduced with PLD2 shRNA. Western blotting was performed with indicated antibodies.

(C) Loss of PLD1/2 increases YAP phosphorylation in HEY cells. PLD1 and PLD2 shRNAs were transduced into HEY cells. Western blotting was performed with indicated antibodies.

(**D** and **E**) Loss of PLD1/2 inhibits YAP downstream gene transcription. The indicated gene transcripts were detected by quantitative PCR in HEK293A cells (**D**) and HEY cells (**E**), and normalized (mean ± s.d., n = 3 biological replicates). As for the PA treatment, PLD1/2 shRNAs-transduced HEY cells were pretreated with 100 μM PA for 2 hours and subjected to quantitative PCR analysis. ** $p < 0.01$. *** $p < 0.001$.

(**F** and **G**) Loss of PLD1/2 induces YAP cytoplasmic translocation in HEY cells. YAP cellular localization was detected by immunofluorescent staining (**F**). Cells from 10 different views (~200 cells) were randomly selected and quantified for YAP localization (**G**). Scale bar, 20 μm.

(**H**) Loss of PLD1/2 increases YAP phosphorylation under Rho-activating conditions. Both control and PLD1/2-deficient HEK293A cells were serum-starved for 24 hours and subjected to the treatment with Rho activator II (1 μg/mL) and TPA (200 nM) for 1 hour. Western blotting was performed with indicated antibodies.

(**I** and **J**) Cellular PA level is controlled by Rho. PA level was examined in both Rho-inactivating conditions (**I**) and Rho-activating conditions (**J**). To inhibit Rho, HEK293A cells were pretreated with C3 (2 μg/mL) for 4 hours or serum starved for 24 hours. To activate Rho, serum-starved HEK293A cells were subjected to the treatment of serum, LPA (1 μM), Rho activator II (1 μg/mL) and TPA (200 nM) for 1 hour, respectively. *** $p < 0.001$.

(**K**) PA treatment stabilizes TAZ but does not affect other Hippo components. HEK293A cells were serum starved for 24 hours and subjected to the indicated lipid (100 μM) treatment for 30 min. Western blotting was performed with indicated antibodies.

Figure S3

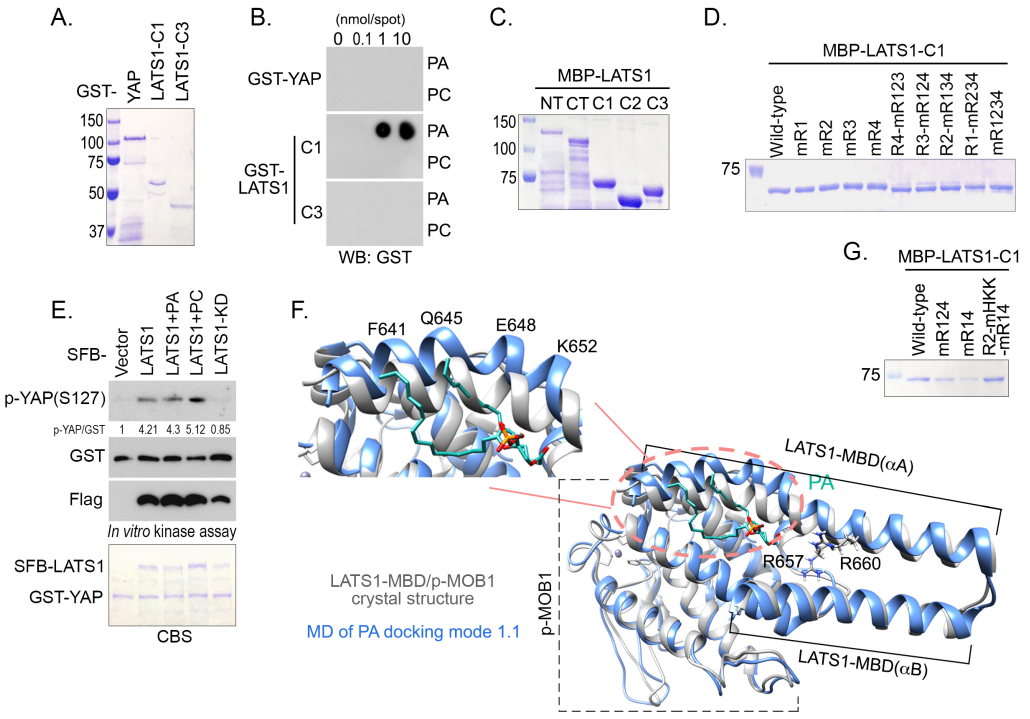

Figure S3. Identification of PA-binding regions in LATS1. (This figure is related to Figures 4 and 5)

(**A** and **B**) PA does not bind YAP. The indicated GST-tagged proteins were purified from bacteria and visualized by coomassie blue staining (**A**). The purified proteins (0.5 μg/mL) were subjected to lipid dot-blot assay. The protein-lipid interaction was detected by Western blotting with GST antibody (**B**).

(**C**) The indicated LATS1 truncation proteins were purified from bacteria and visualized by coomassie blue staining.

(**D**) A series of LATS1-C1 mutant proteins were purified from bacteria and visualized by coomassie blue staining.

(**E**) PA treatment does not affect LATS1 to bind ATP. SFB-LATS1 and its kinase dead mutant (LATS1-KD) were purified from HEK293T cells using S protein beads, washed thoroughly with high-salt buffer containing 250 mM NaCl, and incubated with indicated lipids (300 μM) at 4 ^{0}C overnight. *In vitro* kinase assay was performed using bacterially purified GST-YAP as the substrate. CBS, coomassie blue staining.

(**F**) Superimposition of MD-generated structure of PA/LATS1-MBD/p-MOB1 docking mode 1.1 (colored in blue) to the LATS1-MBD/p-MOB1 crystal structure (colored in gray). PA binding deformed the *N*-terminal part of LATS1-MBD α-helix A. The circled region was enlarged and the representative residues were indicated.

(**G**) The indicated LATS1-C1 mutant proteins were purified from bacteria and visualized by coomassie blue staining.

Figure S4

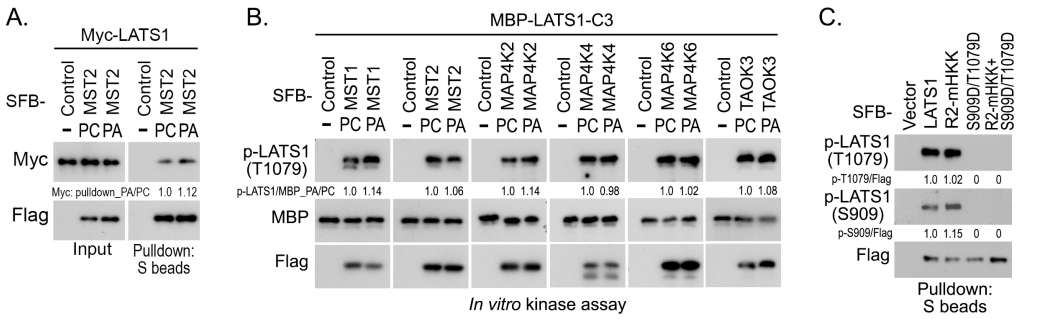

Figure S4. PA treatment does not affect the upstream kinases-mediated LATS phosphorylation. (This figure is related to Figure 6)

(**A**) PA treatment does not affect the association between LATS1 and MST2. HEK293A cells were transfected with the indicated constructs, serum starved for 24 hours, and subjected to the treatment with PC or PA (100 μM) for 30 min. Pulldown assay was performed using S protein beads.

(**B**) PA treatment does not affect the phosphorylation of LATS1-HM as mediated by LATS upstream kinases. The indicated LATS upstream kinases were purified from HEK293T cells using S protein beads, washed thoroughly with high-salt buffer containing 250 mM NaCl, and incubated with indicated lipids (300 μM) at 4 ^{0}C overnight. *In vitro* kinase assay was performed using bacterially purified MBP-LATS1-C3 protein as the substrate. Western blotting was performed with indicated antibodies.

(**C**) LATS1 R2-mHKK mutant can be phosphorylated at S909 and T1079 sites. HEK293A cells were transfected with the indicated constructs, serum starved for 24 hours, and purified using S protein beads. Western blotting was performed with indicated antibodies.

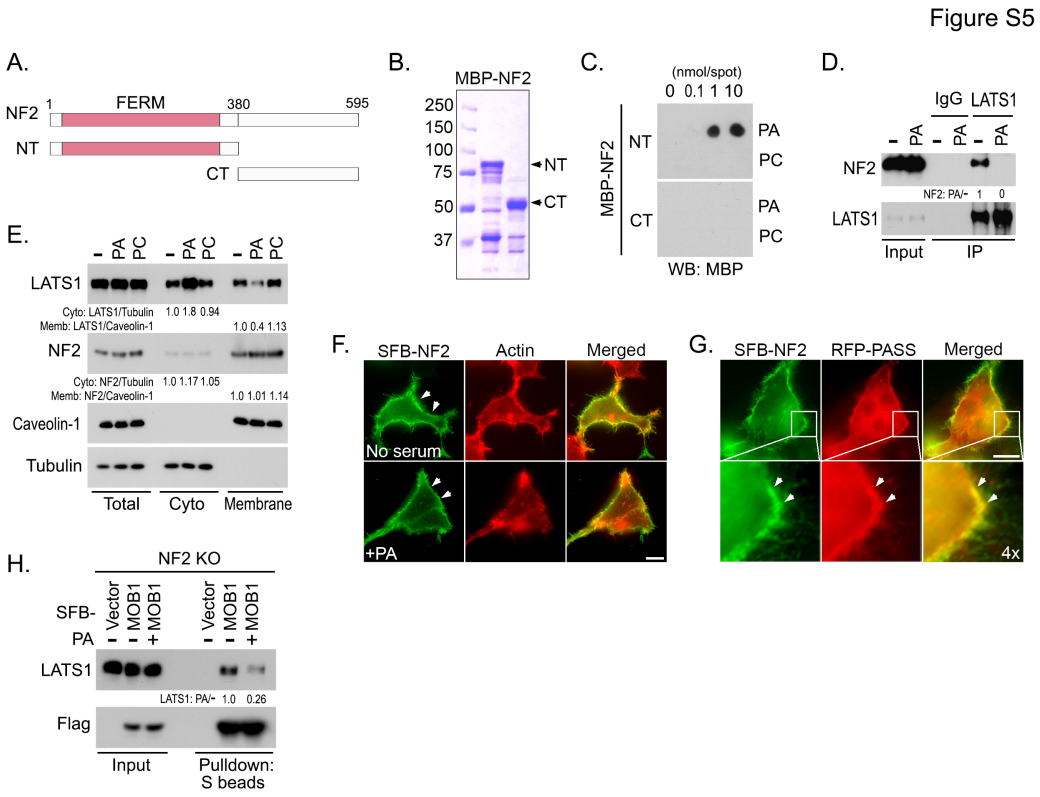

Figure S5. PA interacts with NF2 and inhibits the NF2-mediated LATS membrane translocation and activation. (This figure is related to Figure 6)

(**A**) Schematic illustration of the truncated NF2 proteins used in this study.

(**B** and **C**) PA directly binds *N*-terminus of NF2. The bacterially purified NF2 truncation proteins (**B**) (0.5 μg/mL) were subjected to a lipid dot-blot assay (**C**).

(**D**) PA treatment disrupts the interaction between NF2 and LATS1. Serum-starved HEK293A cells were subjected to PA (100 μM) treatment for 30 min. Immunoprecipitation was performed using LATS1 antibody.

(**E**) PA treatment decreases the level of membrane-associated LATS1. Serum-starved HEK293A cells were treated with PA or PC (100 μM) for 30 min, and subjected to cell fractionation assay.

Western blotting was performed with indicated antibodies. Total, total cell lysates. Cyto, cytoplasm.

(**F**) PA treatment dose not affect NF2 membrane localization. HEK293A cells were transfected with SFB-NF2, serum starved for 24 hours, treated with PA (100 μM) for 30 min, and subjected to immunofluorescent staining. Actin filament was visualized by phalloidin staining. Scale bar, 20 μm. Membrane-localized NF2 was indicated by arrows.

(**G**) NF2 co-localizes with PA on plasma membrane. HEK293A cells were transfected with the indicated constructs and subjected to immunofluorescent staining. The indicated regions in the box are four times enlarged. Co-localization between NF2 and PA sensor was indicated by arrows. Scale bar, 20 μm.

(**H**) PA treatment inhibits LATS1-MOB1 complex formation in NF2 KO cells. NF2 KO HEK293A cells were transfected with the indicated constructs, serum starved for 24 hours, treated with PA (100 μM) for 30 min, and subjected to pulldown assay using S protein beads. Western blotting was performed with indicated antibodies.

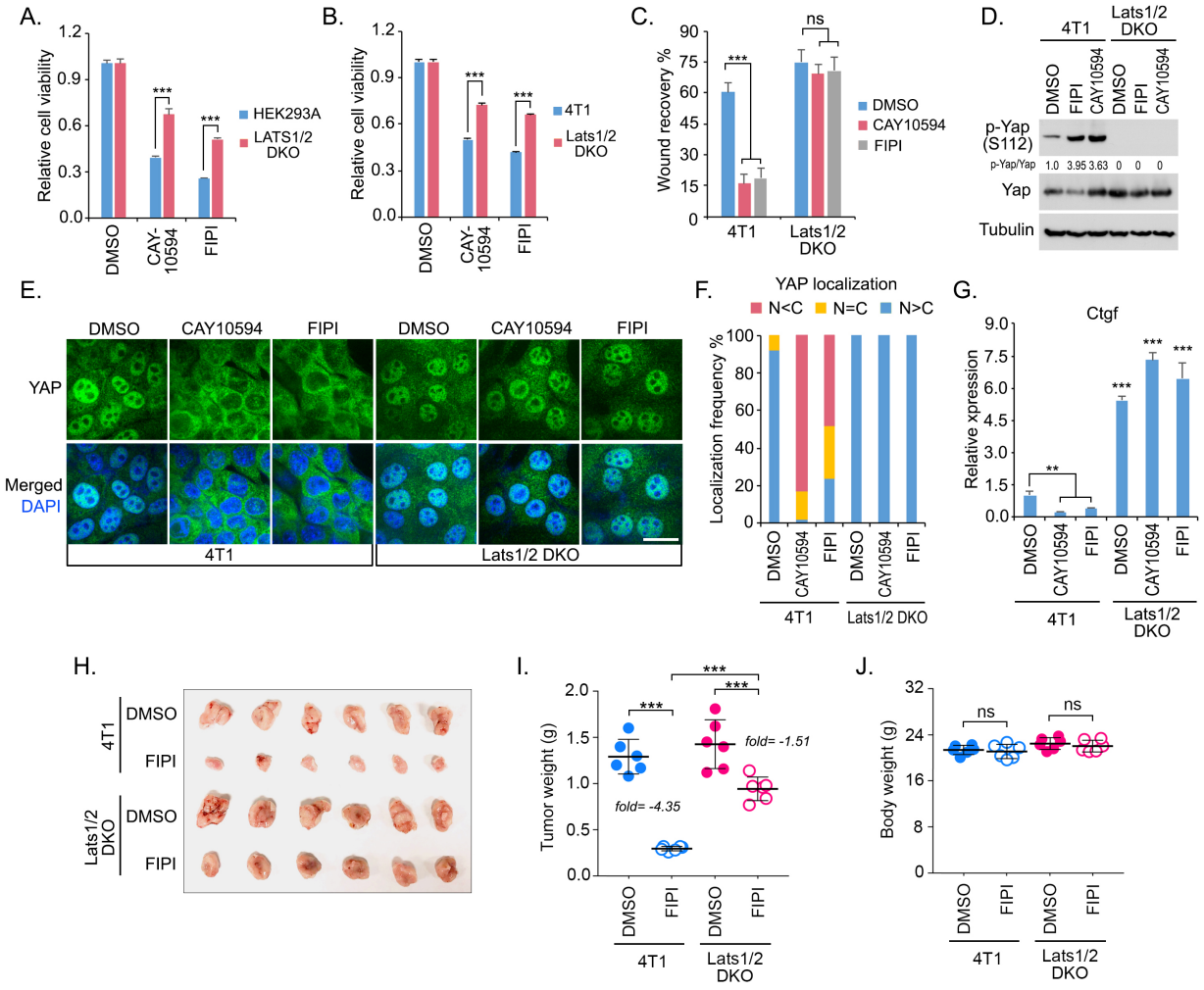

Figure S6. PLD inhibitors target YAP oncogenic activities through LATS. (This figure is related to Figure 7)

(**A**) Loss of LATS1/2 kinases increases the HEK293A cell viability under the PLD inhibitors-treated conditions. Wild-type HEK293A cells and LATS1/2 DKO cells were subjected to the treatment of PLD inhibitors CAY10594 (10 μM) and FIPI (10 μM) for 1 week. Cell viability was normalized (mean ± s.d., n = 3 biological replicates). *** $p < 0.001$.

(**B**) Loss of Lats1/2 kinases increases the 4T1 cell viability under the PLD inhibitors-treated conditions. Wild-type 4T1 cells and Lats1/2 DKO cells were subjected to the treatment of PLD inhibitors CAY10594 (10 μM) and FIPI (10 μM) for 1 week. Cell viability was normalized (mean ± s.d., n = 3 biological replicates). *** $p < 0.001$.

(**C**) Loss of Lats1/2 kinases rescues 4T1 cell migration under the PLD inhibitors-treated conditions. Would healing assay was performed using wild-type 4T1 cells and Lats1/2 DKO cells under the treatment of PLD inhibitors CAY10594 (10 μM) and FIPI (10 μM) for 14 hours. Cell migration was quantified (mean ± s.d., n = 3 biological replicates). *** $p < 0.001$. ns, no significance.

(**D-G**) Loss of Lats1/2 kinases rescues YAP activation under the PLD inhibitors-treated conditions. Wild-type 4T1 and Lats1/2 DKO cells were subjected to the treatment of PLD inhibitors CAY10594 (20 μM) and FIPI (30 μM) for 4 hours. Yap phosphorylation was examined by Western blotting (**D**). Yap cellular localization was examined by immunofluorescent staining (**E**). Cells from 10 different views (~200 cells) were randomly selected and quantified for Yap localization (**F**). Scale bar, 20 μm. The transcription of Yap downstream gene *Ctgf* was detected by quantitative PCR and normalized (mean ± s.d., n = 3 biological replicates) (**G**). ** $p < 0.01$. *** $p < 0.001$.

(**H-J**) Loss of Lats1/2 kinases rescues tumor growth under the PLD inhibitor-treated condition. Wild-type 4T1 and Lats1/2 DKO cells were subjected to xenograft tumor assay and treated with PLD inhibitor FIPI. Xenograft tumors are shown in (**H**). The tumor weight was quantified in (**I**) (n = 6 mice, mean ± s.d.). The corresponding mouse body weight was quantified in (**J**) (n = 6 mice, mean ± s.d.). The FIPI-induced tumor suppression was indicated as the fold change of average tumor weight. *** $p < 0.001$. ns, no significance.

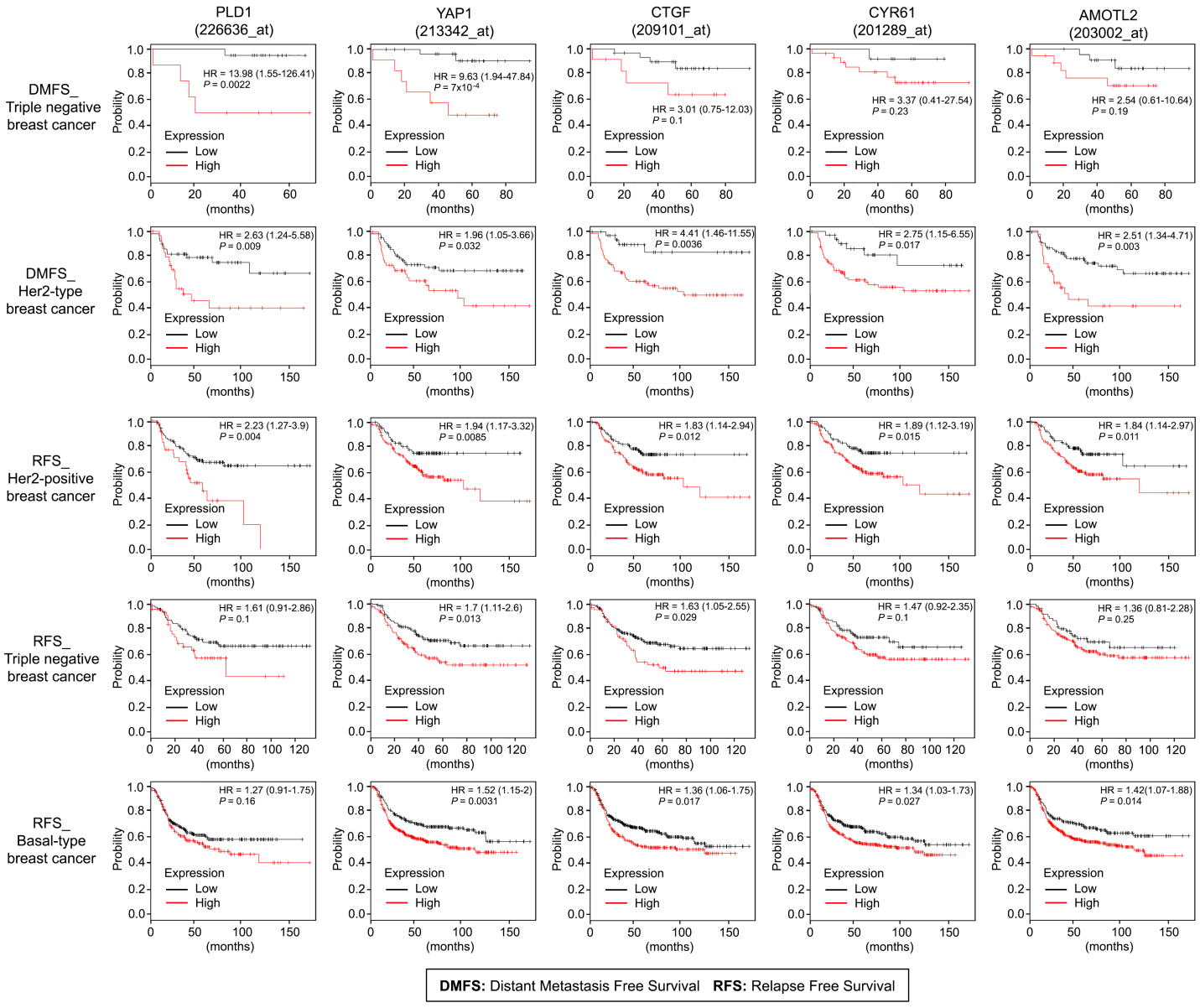

Figure S7. Survival analyses of the PLD-PA-YAP axis in breast cancer patients. (This figure is related to Figure 7)

Kaplan-Meier curves of distant metastasis free survival (DMFS) and relapse free survival (RFS) of breast cancer patients are stratified by PLD1 expression level (probe: 226636_at), YAP1 expression level (probe: 213342_at), CTGF expression level (probe: 209101_at), CYR61 (probe:

201289_at) and AMOTL2 (probe: 203002_at), respectively. Data were obtained from http://kmplot.com/analysis/ and auto select best cutoff was used in the analysis.

Supplementary Table Legend

Table S1. Sequence information of sgRNAs, shRNAs and qPCR primers. (This table is related to STAR Methods)

Sequence information of guide RNAs, shRNAs and qPCR primers used in this study is listed.

Table S1. Sequence information of sgRNAs, shRNAs and qPCR primers

Single-guide RNA	Sequence
NF2_sgRNA	5'-AACCCAAGACGTTCACCGTG-3'
LATS1_sgRNA1	5'-CGTGCAGCTCTCCGCTCTAA-3'
LATS1_sgRNA2	5'-GTTGTGCAGGTGACCATCCA-3'
LATS1_sgRNA3	5'-GTCTCCACATCGACAGCTTG-3'
LATS1_sgRNA4	5'-CCTGTTCGTAGCAACACTTC-3'
LATS1_sgRNA5	5'-ACAGACTGAAGCCATTAGAG-3'
LATS2_sgRNA1	5'-TACGCTGGCACCGTAGCCCT-3'
LATS2_sgRNA2	5'-AGGTAGTCCACGTACGGCCG-3
LATS2_sgRNA3	5'-TTACGCCAGCCTGCCCACGA-3'
LATS2_sgRNA4	5'-CGAAGCTTGGGCCCTCGTAG-3'
LATS2_sgRNA5	5'-GTAGGACGCAAACGAATCGC-3'
MOB1A_sgRNA1	5'-CTATTCTAAAGCGTCTGTTC-3'
MOB1A_sgRNA2	5'-GCAGAAGCAACTCTAGGAAG-3'
MOB1A_sgRNA3	5'-CAAGCTGTTATGTTGCCTGA-3'
MOB1A_sgRNA4	5'-GTTTGAATGTTTTAGAAGAG-3'
MOB1A_sgRNA5	5'-TGTTATGTTGCCTGAGGGAG-3'
MOB1B_sgRNA1	5'-TGGCAGTGGCAACCTTCGGA-3'
MOB1B_sgRNA2	5'-CACTTGGCAGTGGCAACCTT-3'
MOB1B_sgRNA3	5'-TATACTCAAACGCCTCTTTA-3'
MOB1B_sgRNA4	5'-TCATACTGGTGAGAACCCTC-3'
MOB1B_sgRNA5	5'-TCATTGAGATCTTCCCCTTC-3'
RhoA_sgRNA1	5'-ATCGGTATCTGGGTAGGAGA-3'
RhoA_sgRNA2	5'-ATCGACAGCCCTGATAGTTT-3'
RhoA_sgRNA3	5'-TAAACTATCAGGGCTGTCGA-3'
RhoA_sgRNA4	5'-CTGCCTTCTTCAGGTTTCAC-3'
RhoA_sgRNA5	5'-GCTGCTCTGCAAGCTAGACG-3'
PLD1_sgRNA1	5'-TCATAGAAAATCTGGACACG-3'
PLD1_sgRNA2	5'-TTGTGCTTTTATTGGACAGC-3'
PLD1_sgRNA3	5'-GTAAAGACGGATGATCTGAG-3'
PLD1_sgRNA4	5'-GGAACTCCACTTTGAGGGAG-3'
PLD1_sgRNA5	5'-AGTGCAGAGGTATTTACCCG-3'

Short hairpin RNA	Sequence	Sigma-Aldrich cat#:
PLD1_shRNA	5'-GCGTCTACATCCCAACATAAA-3'	TRCN0000001011
PLD2_shRNA	5'-GCCAAGTACAAGACTCCCATA-3'	TRCN0000051149

qPCR primer	Sequence
CTGF-Forward	5'-CCAATGACAACGCCTCCTG-3'
CTGF-Reverse	5'-TGGTGCAGCCAGAAAGCTC-3'
CYR61-Forward	5'-AGCCTCGCATCCTATACAACC-3'
CYR61-Reverse	5'-TTCTTTCACAAGGCGGCACTC-3'
ANKRD1-Forward	5'-CACTTCTAGCCCACCCTGTGA-3'
ANKRD1-Reverse	5'-CCACAGGTTCCGTAATGATTT-3'
AMOTL2-Forward	5'-AGCTTCAATGAGGGTCTGCT-3'
AMOTL2-Reverse	5'-TGAAGGACCTTGATCACTGC-3'
AXIN2-Forward	5'-GTCCAGCAAAACTCTGAGGG-3'
AXIN2-Reverse	5'-CTGGTGCAAAGACATAGCCA-3'
CCND1-Forward	5'-GACCTTCGTTGCCCTCTGT-3'
CCND1-Reverse	5'-TGAGGCGGTAGTAGGACAGG-3'

GLI1-Forward	5'-CCAGACAGAGGCCCACTCTTTT-3'
GLI1-Reverse	5'-TCCGACAGAGGTGAGATGGAC-3'
BCL2-Forward	5'-ATGTGTGTGGAGAGCGTCAA-3'
BCL2-Reverse	5'-GGGCCGTACAGTTCCACAAA-3'
HES1-Forward	5'-ACGTGCGAGGGCGTTAATAC-3'
HES1-Reverse	5'-GGGGTAGGTCATGGCATTGA-3'
HEY-Forward	5'-GGCTCTAGGTTCCATGTCC-3'
HEY-Reverse	5'-CGGCGCTTCTCAATTATTCC-3'
CDKN2B-Forward	5'-AATCTTCCGATGGATGAATCTC-3'
CDKN2B-Reverse	5'-GTGCTAATCACTGCCTTCTC-3'
CDKN1A-Forward	5'-TGTCCGTCAGAACCCATGC-3'
CDKN1A-Reverse	5'-AAAGTCGAAGTTCCATCGCTC-3'
GAPDH-Forward	5'-ATGGGGAAGGTGAAGGTCG-3'
GAPDH-Reverse	5'-GGGGTCATTGATGGCAACAATA-3'
Ctgf-Forward	5′-CAAGGACCGCACAGCAGTT-3′
Ctgf-Reverse	5′-AGAACAGGCGCTCCACTCTG-3′
Gapdh-Forward	5′-TGTTCCTACCCCCAATGTGT-3′
Gapdh-Reverse	5′-TGTGAGGGAGATGCTCAGTG-3′